

First principles study on the spin transfer torques

Shuai Wang, Yuan Xu, and Ke Xia

*State Key Laboratory for Surface Physics, Institute of Physics,
Chinese Academy of Sciences, P.O. Box 603, Beijing 100080, China*

(Dated: October 30, 2018)

An efficient first principles method was developed to calculate spin transfer torques in layered system with noncollinear magnetization. The complete scattering wave function is determined by matching the wave function in the scattering region with the Bloch states in the leads. The spin transfer torques are obtained with aid of the scattering wave function. We applied our method to the ferromagnetic spin valve and found that the material (Co, Ni and Ni₈₀Fe₂₀) dependence of the spin transfer torques could be well understood by the Fermi surface. Ni has much longer spin injection penetration length than Co. Interfacial disorder is also considered. It is found that the spin transfer torques could be enhanced by the interfacial disorder in some system.

PACS numbers: 72.25.Ba, 85.75.-d, 72.10.Bg

I. INTRODUCTION

Spin angular momentum can be transferred by the flowing electrons from one ferromagnetic (FM) material to another FM material, which is so-called spin transfer torques (STT) introduced by Slonczewski¹ and Berger². Those two seminal studies have shown that the dynamics of magnetization in FM material could be dominated by the spin torques carried by electric current. The excitation of coherent precession of magnetization and spin wave were predicted. The STT was soon identified in the experiments³ by clear observation of the magnetization switching in FM spin valve, which excites great interests in experiment and theory^{4,5,6,7,8,9,10,11}.

The theories^{6,7,8,9} combining the quantum treatment of the interface scattering and the Boltzmann-like treatment of the bulk scattering work reasonable well with the experiments of metallic system. However, recent experiments on the tunnelling system¹² and magnetic domain wall¹³ call for a full quantum treatment of the whole system. Edwards *et.al.*,¹⁰ obtained the torques of spin valve in the empirical tight-binding frame and Haney *et.al.*,¹¹ calculated the torques in the similar structure with nonequilibrium Green's function (NEGF) based on LCAO basis.

Both semiclassical and quantum mechanical study show that the STT is most significant near the nonmagnet(NM)|FM interfaces in the spin valve. Up to now, only a few studies have addressed the material dependence of spin torque, which could be an important issue as the spin dependent transport is greatly affected by the electronic structure in FM^{14,15}. Furthermore, previous studies focused on ideal structure without considering the disorder at the FM|NM interface, which should exist in the realistic spin valve¹⁶.

The main aim of this paper is to formulate a method to calculate STT of a noncollinear magnetized system within the first principles frame. Differing from the previous Green function based work¹¹, we obtained the complete scattering wave functions of the whole system¹⁷. The STT⁹ is formulated in the tight-binding represen-

tation. Large system such as domain wall can be well treated in this framework¹⁸. We apply our formalism to the Co|Cu|FM|Cu spin valve system with impurity scattering at the FM|NM interface. Our study shows that the STT can penetrate deep into the ferromagnetic materials for Ni, which is quite different from Co. It is also found that average torques are enhanced in the presence of interfacial disorder.

This paper is organized as following. In Sec. II, we present the details of the formalism for constructing the eigenmodes of the lead and computing the STT in spin valve. Note that not only the transmission and reflection coefficient are obtained but also the wave function in the scattering regime is obtained explicitly. In Section III, the method is used to calculate the conductance and STT in the systems of Co|Cu|FM|Cu(111), with FM is Co, Ni and Ni₈₀Fe₂₀, respectively. The effect of interfacial disorder is discussed. In Sec. IV, we summarize our results.

II. THEORETICAL MODEL

Let us focus on the spin transport and STT in the layered systems sketched in Fig.1. The scattering region **S**, which is denoted by the layer index $1 \leq I \leq N$, is sandwiched by left(**L**) and right(**R**) leads. For this device, there exists perfect lattice periodicity in the *X-Z* plane. Particle current flows along *Y* axis. In scattering region no periodicity is assumed along current direction. Here the atomic potentials were determined by the tight-binding linearized muffin-tin-orbital (TB-LMTO) surface Green's function (SGF) method¹⁹. When combined with the coherent potential approximation (CPA), this method allows the electronic structure, charge, and spin densities of layered materials with substitutional disorder to be calculated self-consistently with high efficiency. To model the noncollinear system in the spin valve, the rigid potential approximation is used. In this approximation, we rotate the potential of fixed magnet in spin space to construct the relative angle between the

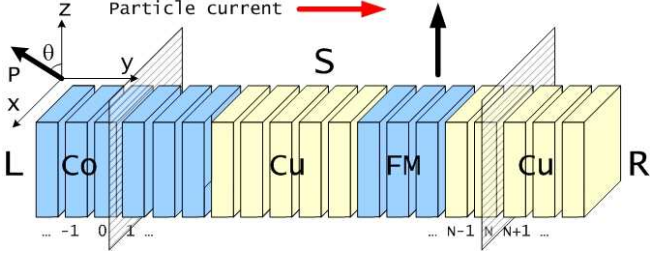


FIG. 1: (color online) Sketch of the configuration used for current-induced switching. A scattering region is sandwiched by left-(L) and right-hand(R) leads which have translational symmetry and are partitioned into principle layers perpendicular to the transport direction. The scattering region contains N principle layers but the structure and chemical composition are in principle arbitrary. The switching layer FM can be Co, Ni, Ni₈₀Fe₂₀.

polarization directions of fixed magnet and free magnet, which is a good approximation as the two magnets are spaced far enough by a Cu layer.

Following previous work¹⁷, we describe the theoretical frame developed with wave-function matching (WFM) based on TB-LMTO basis for studying the STT. In Sec. II A, we review the Hamiltonian and KKR equation for a device with noncollinear magnetization. The equation of motion (EOM) for layered system is extracted from KKR equation. In the Sec. II B, the boundary conditions of the EOM are formulated in terms of the Bloch states in the leads. In the Sec. II C, by solving the EOM in the scattering region with embedding potentials of the two leads, we obtain the complete scattering wave function of the scattering region. In the Sec. II D and E, the particle current and spin current are formulated with those obtained scattering wave function expanded in TB-LMTO basis.

A. Hamiltonian and KKR equation

For layered systems, atoms can always be grouped into principle layers defined as to be so thick that the interactions between layers I and $I \pm 2$ are negligible as shown in Fig.1.

The EOM for I th principal layer can be written as

$$\mathbf{H}_{I,I-1}\mathbf{a}_{I-1} + (\mathbf{H} - E)_{II}\mathbf{a}_I + \mathbf{H}_{I,I+1}\mathbf{a}_{I+1} = 0, \quad (1)$$

where E is always set to the Fermi energy E_F for the transport problem. Here, \mathbf{a}_I is the a vector describing the amplitudes of the I th layer in terms of the localized orbital basis $|\mathbf{R}L\zeta\rangle$, where \mathbf{R} is the site index and L can be defined by $L \equiv (l, m)$. l and m are the azimuthal and magnetic quantum numbers respectively. $\zeta = \uparrow (\downarrow)$ denotes that the basis is eigenstate in spin space, which is parallel (antiparallel) to spin quantization axis.

To the first order approximation of the full LMTO Hamiltonian, a short-range TB-LMTO Hamiltonian in

the α representation^{20,21} in the global coordinate system can be written as

$$\begin{aligned} \mathbf{H}_{\mathbf{R}L,\mathbf{R}'L'}^\alpha &= U_{\mathbf{R}}\bar{\mathcal{C}}_{\mathbf{R}L}^\alpha U_{\mathbf{R}}^\dagger \delta_{\mathbf{R}'L'/\mathbf{R}L} \\ &+ [U_{\mathbf{R}}(\bar{\Delta}_{\mathbf{R}L}^\alpha)^{\frac{1}{2}} U_{\mathbf{R}}^\dagger S_{\mathbf{R}L,\mathbf{R}'L'}^\alpha \\ &\times U_{\mathbf{R}'}(\bar{\Delta}_{\mathbf{R}'L'}^\alpha)^{\frac{1}{2}} U_{\mathbf{R}'}^\dagger], \end{aligned} \quad (2)$$

where $\bar{\mathcal{C}}_{\mathbf{R}L}^\alpha$ and $\bar{\Delta}_{\mathbf{R}L}^\alpha$ are 2×2 potential parameter matrices expanded in spin space and diagonal in the local coordinate system. The unitary rotation matrix at site \mathbf{R} can be defined by

$$U_{\mathbf{R}}(\theta_{\mathbf{R}}, \varphi_{\mathbf{R}}) = \begin{bmatrix} \cos \frac{\theta_{\mathbf{R}}}{2} e^{-i\frac{\varphi_{\mathbf{R}}}{2}} & -\sin \frac{\theta_{\mathbf{R}}}{2} e^{-i\frac{\varphi_{\mathbf{R}}}{2}} \\ \sin \frac{\theta_{\mathbf{R}}}{2} e^{i\frac{\varphi_{\mathbf{R}}}{2}} & \cos \frac{\theta_{\mathbf{R}}}{2} e^{i\frac{\varphi_{\mathbf{R}}}{2}} \end{bmatrix}, \quad (3)$$

where $\theta_{\mathbf{R}}, \varphi_{\mathbf{R}}$ are the azimuth angles of the local quantization axis. Screened structure constants $S_{\mathbf{R}L,\mathbf{R}'L'}^\alpha$ contain all information about the structure, which are block diagonal in the spin space,

$$S_{\mathbf{R}L,\mathbf{R}'L'}^\alpha = \begin{bmatrix} s_{\mathbf{R}L,\mathbf{R}'L'}^\alpha & 0 \\ 0 & s_{\mathbf{R}L,\mathbf{R}'L'}^\alpha \end{bmatrix}. \quad (4)$$

Note that $s_{\mathbf{R}L,\mathbf{R}'L'}^\alpha$ is spin independent. The Hamiltonian of Eq.(2) yields eigenvalues corrected to first order in $(E - E_F)$ and is exact when we set $E = E_F$.

For a noncollinear magnetized system, the "tail-cancellation" condition yields the KKR equation²¹,

$$\sum_{\mathbf{R}',L'} \left(-U_{\mathbf{R}}\bar{\mathcal{P}}_{\mathbf{R}L}^\alpha(E) U_{\mathbf{R}}^\dagger \delta_{\mathbf{R}\mathbf{R}'} \delta_{L'L'} - S_{\mathbf{R}L,\mathbf{R}'L'}^\alpha \right) C_{\mathbf{R}'L'} = 0, \quad (5)$$

where $\mathbf{C}_{\mathbf{R}L} = (\mathbf{C}_{\mathbf{R}L\uparrow}, \mathbf{C}_{\mathbf{R}L\downarrow})^T$ has the relation to the wave amplitude $\mathbf{a}_{\mathbf{R}L}$ of L orbital at site \mathbf{R} as $\mathbf{C}_{\mathbf{R}L} = U_{\mathbf{R}}(\bar{\Delta}_{\mathbf{R}L}^\alpha)^{\frac{1}{2}} U_{\mathbf{R}}^\dagger \mathbf{a}_{\mathbf{R}L}$. $\bar{\mathcal{P}}_{\mathbf{R}L}^\alpha(E)$ is the screened potential function matrix and contains all information about the atomic species at site \mathbf{R} for calculating the electronic structure. It is diagonal in the local coordinate system,

$$\bar{\mathcal{P}}_{\mathbf{R}L}^\alpha(E) \equiv \begin{bmatrix} \bar{\mathcal{P}}_{\mathbf{R}L}^{\alpha,\uparrow} & 0 \\ 0 & \bar{\mathcal{P}}_{\mathbf{R}L}^{\alpha,\downarrow} \end{bmatrix}, \quad (6)$$

where $\bar{\mathcal{P}}_{\mathbf{R}L}^{\alpha,\uparrow(\downarrow)} \equiv (E - \bar{\mathcal{C}}_{\mathbf{R}L}^{\alpha,\uparrow(\downarrow)}) (\bar{\Delta}_{\mathbf{R}L}^{\alpha,\uparrow(\downarrow)})^{-1}$ and E is set to E_F for the transport problem we considered.

As there exists two-dimensional translational symmetry in the lateral plane, the states along the transport direction can be characterized by a lateral wave vector \mathbf{k}_{\parallel} in the corresponding 2-dimensional Brillouin zone (2D BZ). The screened KKR equation in the mixed representation of \mathbf{k}_{\parallel} can be expressed in terms of principal layers as,

$$-S_{I,I-1}^{\mathbf{k}_{\parallel}} \mathbf{C}_{I-1}(\mathbf{k}_{\parallel}) + \left(U_I \bar{P}_{I,I}(E_F) U_I^\dagger - S_{I,I}^{\mathbf{k}_{\parallel}} \right) \mathbf{C}_I(\mathbf{k}_{\parallel}) - S_{I,I+1}^{\mathbf{k}_{\parallel}} \mathbf{C}_{I+1}(\mathbf{k}_{\parallel}) = 0, \quad (7)$$

where $\mathbf{C}_I(\mathbf{k}_{\parallel})$ is the wave vector describing the wave function amplitudes of the I th principal layer consisting of h atom sites and has the dimension of $2(l_{\max} + 1)^2 h = 2M$. $\bar{P}_{I,I}$ is $2M \times 2M$ diagonal matrix. and $S_{I,I}^{\mathbf{k}_{\parallel}}$ is also $2M \times 2M$ matrices with its sub matrix $S_{\mathbf{R}L, \mathbf{R}'L'}^{\mathbf{k}_{\parallel}}$ defined by

$$S_{\mathbf{R}L, \mathbf{R}'L'}^{\mathbf{k}_{\parallel}} = \sum_{\mathbf{T}_{\parallel}} \exp[i\mathbf{k}_{\parallel} \cdot \mathbf{T}_{\parallel}] S_{\mathbf{R}L, (\mathbf{R}'+\mathbf{T}_{\parallel})L'}^{\alpha} \quad \begin{matrix} \mathbf{R} \in I \\ \mathbf{R}'+\mathbf{T}_{\parallel} \in I' \end{matrix} \quad (8)$$

where I and I' are layer index and \mathbf{T}_{\parallel} is 2-dimensional translational vector in the plane of principal layer.

Note that Eq.(7) is the EOM by analogy with Eq.(1). We will solve it for a given energy E_F of electrons to obtain the wave function of the scattering state. The reference to \mathbf{k}_{\parallel} and E_F in the formulism will be suppressed in the following two parts Sec. II B and Sec. II C.

B. Eigenmodes of the leads

For the scattering problem, far enough away from the scattering region the wave function can be expressed rigorously with asymptotic forms in terms of reflection and transmission coefficients and Bloch states in the leads. As the wave function should satisfy Bloch's theorem in a periodic potential, we set $\bar{\mathbf{C}}_n = \lambda^n \bar{\mathbf{C}}_0$. In local coordinate system, the EOM in lead becomes

$$\begin{pmatrix} S_{0,1}^{-1} (\bar{P}_{00} - S_{0,0}) & -S_{0,1}^{-1} S_{1,0} \\ 1 & 0 \end{pmatrix} \begin{pmatrix} \bar{\mathbf{C}}_0 \\ \bar{\mathbf{C}}_{-1} \end{pmatrix} = \lambda \begin{pmatrix} \bar{\mathbf{C}}_0 \\ \bar{\mathbf{C}}_{-1} \end{pmatrix}. \quad (9)$$

Details for solving Bloch states $\bar{\mathbf{C}}_0$ can be found in Ref.[17]. To overcome the numerical difficult of the spin degeneracy in NM lead and reduce the calculation efforts, we solve the EOM in the leads in local coordinate system for each spin separately. In global coordinate system, Bloch states can be obtained after an unitary transformation. For the amplitude of 0th layer, we have $\mathbf{C}_0 = U_0 \bar{\mathbf{C}}_0$.

The propagating states and evanescent states can be identified and sorted into right-going(+) or left-going(-). Letting $\bar{\mathbf{w}}_{\mu}^{\uparrow(\downarrow)}(\pm)$ denotes the solutions of $\bar{\mathbf{C}}$ corresponding to eigenvalue $\lambda_{\mu}(\pm)$, where $\uparrow(\downarrow)$ denotes the eigenstate parallel (antiparallel) to the local spin quantization direction. Constructing the matrix $\mathbf{W}(\pm)$ as

$$\begin{aligned} \mathbf{W}(\pm) &= U_0 \bar{\mathbf{W}}(\pm) \\ &\equiv U_0 [\bar{\mathbf{w}}_1^{\uparrow}(\pm), \dots, \bar{\mathbf{w}}_M^{\uparrow}(\pm), \\ &\quad \bar{\mathbf{w}}_1^{\downarrow}(\pm), \dots, \bar{\mathbf{w}}_M^{\downarrow}(\pm)]. \end{aligned} \quad (10)$$

Following Ando²², define the Bloch factor as

$$F(\pm) \equiv \mathbf{W}(\pm) \mathbf{\Lambda}(\pm) \mathbf{W}^{-1}(\pm). \quad (11)$$

where $\mathbf{\Lambda}(\pm)$ is a diagonal matrix with the diagonal elements given by $[\lambda_1^{\uparrow}(\pm), \dots, \lambda_M^{\uparrow}(\pm), \lambda_1^{\downarrow}(\pm), \dots, \lambda_M^{\downarrow}(\pm)]$. In local coordinate system, we have the relation $\bar{\mathbf{C}}_I(\pm) = \bar{F}^{I-J}(\pm) \bar{\mathbf{C}}_J(\pm)$ ¹⁷. It is easy to proof that the Bloch factor defined above satisfies the Bloch relation in global coordinate system

$$\mathbf{C}_I(\pm) = F(\pm)^{I-J} \mathbf{C}_J(\pm). \quad (12)$$

Bloch factors matrix $F(\pm)$ relates the wave amplitude in the I th layer to that in the J th layer for a state in the lead.

C. Scattering problem

The equations of motion with open boundary conditions for a device usually contain infinite number of equations. By incorporating the boundary conditions in the leads, the scattering problem can be reduced to a set of coupled linear equations with finite number of equations¹⁷.

For an electron coming from the left lead, Eq.(7) for $I = 0$ can be rewritten as

$$\begin{aligned} &(U_0 \bar{P}_{0,0} U_0^\dagger - \tilde{S}_{0,0}) \mathbf{C}_0 - S_{0,1} \mathbf{C}_1 \\ &= S_{0,-1} [F_L^{-1}(+) - F_L^{-1}(-)] \mathbf{C}_0(+), \end{aligned} \quad (13)$$

where L denotes the left lead and with $\tilde{S}_{0,0} \equiv S_{0,0} + S_{0,-1} F_L^{-1}(-)$. The $S_{0,-1} F_L^{-1}(-)$ is the embedding potential for the left lead.

In the right lead, only right-going waves exist in the $(N+1)$ th layer. The EOM for $I = N+1$ is

$$(U_{N+1} \bar{P}_{N+1, N+1} U_{N+1}^\dagger - \tilde{S}_{N+1, N+1}) \mathbf{C}_{N+1} - S_{N+1, N} \mathbf{C}_N = 0, \quad (14)$$

where $\tilde{S}_{N+1, N+1} = S_{N+1, N+1} + S_{N+1, N+2} F_R(+)$ and $S_{N+1, N+2} F_R(+)$ is the embedding potential for the right lead.

Making use of the lead boundary conditions for 0th and $(N + 1)$ layer, the scattering wave function can be found as

$$\begin{pmatrix} \mathbf{C}_0 \\ \mathbf{C}_1 \\ \mathbf{C}_2 \\ \vdots \\ \mathbf{C}_N \\ \mathbf{C}_{N+1} \end{pmatrix} = (U\bar{\mathbf{P}}U^\dagger - \tilde{\mathbf{S}})^{-1} \times \begin{pmatrix} S_{1,-1} [F_L^{-1}(+) - F_L^{-1}(-)] \mathbf{C}_0(+) \\ 0 \\ \vdots \\ 0 \\ 0 \end{pmatrix}, \quad (15)$$

where $\tilde{\mathbf{S}}$ is of block tridiagonal matrix containing $S_{I,J}$ except the $\tilde{S}_{0,0}$ and $\tilde{S}_{N+1,N+1}$ are defined as above. The spin polarization direction at different sites can be incorporated by the unitary rotation U at corresponding site.

To obtain the scattering state, we need to specify an incoming state $\mathbf{C}_0(+)$ at the right side of Eq.(15). This can be achieved by introducing the right going eigenmodes of left lead as the incoming states by setting $\mathbf{C}_0(+)$ to be $\mathbf{w}_\lambda(+)$, where $\mathbf{w}_\lambda(+)$ should be renormalized so as to carry an unit flux. Each $\mathbf{w}_\lambda(+)$ corresponds to a scattering state in device.

The amplitude of layers from 0 to $N + 1$ solved from Eq.(15) serves for computing the particle current and spin current. Also, the scattering matrix can be obtained¹⁷.

D. Particle Current

Let us consider the particle current operator of a quasi one-dimensional TB model for a special \mathbf{k}_\parallel vector at $E = E_F$. The MTO-basis functions $|\mathbf{R}L\zeta^{\mathbf{k}_\parallel}\rangle$ are obtained from the Bloch sum of the particle waves:

$$|\mathbf{R}L\zeta^{\mathbf{k}_\parallel}\rangle = \sum_{T_\parallel} e^{i\mathbf{k}_\parallel \cdot \mathbf{T}_\parallel} |\mathbf{R} + \mathbf{T}_\parallel, L\zeta^\alpha\rangle. \quad (16)$$

So the density operator at \mathbf{R} site in the mixed representation for a special \mathbf{k}_\parallel vectors can be defined by

$$\hat{\rho}_{\mathbf{R}}^{\mathbf{k}_\parallel} \equiv \sum_{L\zeta} |\mathbf{R}L\zeta^{\mathbf{k}_\parallel}\rangle \langle \mathbf{R}L\zeta^{\mathbf{k}_\parallel}|. \quad (17)$$

Neglecting the electron motion inside the atomic cells, the velocity operators can be expressed by the intersite hopping²³ and will give the total current for subspace. The velocity (current) operator can be defined by

$$\hat{\mathbf{V}} = \frac{1}{i\hbar} [\hat{\mathbf{X}}, \hat{\mathbf{H}}], \quad (18)$$

where $\hat{\mathbf{X}}$ is the coordinate operator, which can be represented in TB model by a diagonal matrix $\hat{\mathbf{X}}_{\mathbf{R}\mathbf{L},\mathbf{R}'\mathbf{L}'} = \mathbf{X}_{\mathbf{R}}\delta_{\mathbf{R}\mathbf{R}'}\delta_{\mathbf{L}\mathbf{L}'}$ ²³.

With aid of Eq.(18), the current operator $\hat{\mathbf{J}}_{\mathbf{R}'\mathbf{R}}^{\mathbf{k}_\parallel}$ from \mathbf{R}' th to \mathbf{R} th site ($\mathbf{R} \neq \mathbf{R}'$) can be written as

$$\hat{\mathbf{J}}_{\mathbf{R}'\mathbf{R}}(\mathbf{k}_\parallel) = \sum_{\mathbf{L}\mathbf{L}'} \frac{1}{i\hbar} [\hat{\mathbf{H}}_{\mathbf{R}\mathbf{L},\mathbf{R}'\mathbf{L}'}^{\mathbf{k}_\parallel} - h.c.]. \quad (19)$$

where $\hat{\mathbf{H}}_{\mathbf{R}\mathbf{L}\zeta,\mathbf{R}'\mathbf{L}'\zeta'}^{\mathbf{k}_\parallel} = |\mathbf{R}\mathbf{L}\zeta^{\mathbf{k}_\parallel}\rangle \mathbf{H}_{\mathbf{R}\mathbf{L}\zeta,\mathbf{R}'\mathbf{L}'\zeta'}^{\mathbf{k}_\parallel} \langle \mathbf{R}'\mathbf{L}'\zeta'^{\mathbf{k}_\parallel}|$ and $\mathbf{H}_{\mathbf{R}\mathbf{L},\mathbf{R}'\mathbf{L}'}^{\mathbf{k}_\parallel}$ is the Hamiltonian matrix in spin space, which has relation with Eq.(2) as

$$\mathbf{H}_{\mathbf{R}\mathbf{L},\mathbf{R}'\mathbf{L}'}^{\mathbf{k}_\parallel} = \sum_{\mathbf{T}_\parallel} \exp[i\mathbf{k}_\parallel \cdot \mathbf{T}_\parallel] \mathbf{H}_{\mathbf{R}\mathbf{L},(\mathbf{R}'+\mathbf{T}_\parallel)\mathbf{L}'}^\alpha. \quad (20)$$

The expectation value of operator $\hat{\mathbf{A}}$ is $\langle \hat{\mathbf{A}} \rangle \equiv \langle \Psi | \hat{\mathbf{A}} | \Psi \rangle$. The particle current can be expressed as

$$\langle \hat{\mathbf{J}}_{\mathbf{R}'\mathbf{R}}(\mathbf{k}_\parallel) \rangle = \sum_{\mathbf{L}\mathbf{L}'} \frac{1}{i\hbar} [a_{\mathbf{R}\mathbf{L}}^\dagger(\mathbf{k}_\parallel) \mathbf{H}_{\mathbf{R}\mathbf{L},\mathbf{R}'\mathbf{L}'}^{\mathbf{k}_\parallel} \mathbf{a}_{\mathbf{R}'\mathbf{L}'}(\mathbf{k}_\parallel) - h.c.], \quad (21)$$

where where $\mathbf{a}_{\mathbf{R}\mathbf{L}}(\mathbf{k}_\parallel) = (\mathbf{a}_{\mathbf{R}\mathbf{L}\uparrow}(\mathbf{k}_\parallel), \mathbf{a}_{\mathbf{R}\mathbf{L}\downarrow}(\mathbf{k}_\parallel))^T$, and $\mathbf{a}_{\mathbf{R}\mathbf{L}\zeta}(\mathbf{k}_\parallel) = \langle \mathbf{R}\mathbf{L}\zeta^{\mathbf{k}_\parallel} | \Psi \rangle$. $\mathbf{a}_{\mathbf{R}\mathbf{L}}(\mathbf{k}_\parallel)$ has the relation with $\mathbf{C}_{\mathbf{R}\mathbf{L}}(\mathbf{k}_\parallel)$ as follow

$$\mathbf{a}_{\mathbf{R}\mathbf{L}}(\mathbf{k}_\parallel) = U_{\mathbf{R}} (\bar{\Delta}_{\mathbf{R}\mathbf{L}}^\alpha)^{-\frac{1}{2}} U_{\mathbf{R}}^\dagger \mathbf{C}_{\mathbf{R}\mathbf{L}}(\mathbf{k}_\parallel). \quad (22)$$

The $\mathbf{C}_{\mathbf{R}\mathbf{L}}(\mathbf{k}_\parallel)$ can be obtained by Eq.(15) for a given \mathbf{k}_\parallel . Within the MTO formulism, the current can also be expressed with structure constants matrix as in Ref.17

$$\langle \hat{\mathbf{J}}_{\mathbf{R}'\mathbf{R}}(\mathbf{k}_\parallel) \rangle = \sum_{\mathbf{L}\mathbf{L}'} \frac{1}{i\hbar} [\mathbf{C}_{\mathbf{R}\mathbf{L}}^\dagger(\mathbf{k}_\parallel) S_{\mathbf{R}\mathbf{L},\mathbf{R}'\mathbf{L}'}^{\mathbf{k}_\parallel} \mathbf{C}_{\mathbf{R}'\mathbf{L}'}(\mathbf{k}_\parallel) - h.c.]. \quad (23)$$

The continuity equation of particle current at \mathbf{R} site in the I th principle layer reads

$$\begin{aligned} & \sum_{\mathbf{R}' \in I-1, I} \langle \hat{\mathbf{J}}_{\mathbf{R}',\mathbf{R}}(\mathbf{k}_\parallel) \rangle - \sum_{\mathbf{R}' \in I, I+1} \langle \hat{\mathbf{J}}_{\mathbf{R},\mathbf{R}'}(\mathbf{k}_\parallel) \rangle \\ &= \frac{d \langle \hat{\rho}_{\mathbf{R}}^{\mathbf{k}_\parallel} \rangle}{dt}, \end{aligned} \quad (24)$$

where the first term at the left side of Eq.(24) is the incoming current to the \mathbf{R} site and the second term is outgoing current from this site.

As shown in Fig.(2), the current is assumed to flow from $I - 1$ th layer to $I + 1$ th layer. Considering the \mathbf{R} site, the incoming current is composed of current from the sites in the $I - 1$ th layer and the sites ahead \mathbf{R} site (relative to transport direction) in I th layer. If there exist other atoms in the same plane of \mathbf{R} (see Fig.(2)), the current from those atoms also are considered as the component of incoming current to \mathbf{R} site. The outgoing current is composed of current to the sites in $I + 1$ th layer

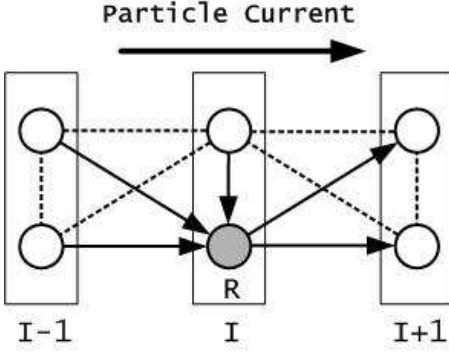


FIG. 2: Illustration of incoming current and outgoing current for the \mathbf{R} th site. Assuming the particle current comes from $I - 1$ th layer to $I + 1$ th layer. Arrow lines denote the current related to \mathbf{R} th site and dot lines denote the coupling between sites irrelevant to \mathbf{R} th site.

and those sites behinds \mathbf{R} site in I th layer. Note that treating the current between atoms in the same plane as the incoming current or outgoing current will not result in any physical consequence. Careful check has been carried out that the particle current conservation law can be satisfied atom by atom and layer by layer. For the scattering states we calculated, the right side of the Eq.(24) is zero.

In the linear response regime, the particle current under a small bias V_b at zero temperature can be expressed as²⁴,

$$\mathbf{J}_{\mathbf{R}\mathbf{R}'} = \frac{e}{h} \frac{1}{N_{\parallel}} \sum_{\mathbf{k}_{\parallel}} \langle \hat{\mathbf{J}}_{\mathbf{R}\mathbf{R}'}(\mathbf{k}_{\parallel}) \rangle V_b, \quad (25)$$

$$\langle \hat{\mathcal{J}}_{\mathbf{R}',\mathbf{R}}(\mathbf{k}_{\parallel}) \rangle = \sum_{LL'} \frac{1}{2i\hbar} \left[\mathbf{a}_{\mathbf{R}L}^{\dagger}(\mathbf{k}_{\parallel}) \hat{\sigma} \mathbf{H}_{\mathbf{R}L,\mathbf{R}'L'}^{\mathbf{k}_{\parallel}} \mathbf{a}_{\mathbf{R}'L'}(\mathbf{k}_{\parallel}) + \mathbf{a}_{\mathbf{R}L}^{\dagger}(\mathbf{k}_{\parallel}) \mathbf{H}_{\mathbf{R}L,\mathbf{R}'L'}^{\mathbf{k}_{\parallel}} \hat{\sigma} \mathbf{a}_{\mathbf{R}'L'}(\mathbf{k}_{\parallel}) - h.c. \right]. \quad (29)$$

The STT $\langle \hat{\mathbf{T}}_{\mathbf{R}}^s(\mathbf{k}_{\parallel}) \rangle$ can be defined as the difference of the incoming spin current and outgoing spin current of \mathbf{R} site in the I th principal layer:

$$\begin{aligned} & \langle \hat{\mathbf{T}}_{\mathbf{R}}^s(\mathbf{k}_{\parallel}) \rangle \\ &= \sum_{\mathbf{R}' \in I-1, I} \langle \hat{\mathcal{J}}_{\mathbf{R}',\mathbf{R}}^s(\mathbf{k}_{\parallel}) \rangle - \sum_{\mathbf{R}' \in I, I+1} \langle \hat{\mathcal{J}}_{\mathbf{R},\mathbf{R}'}^s(\mathbf{k}_{\parallel}) \rangle. \end{aligned} \quad (30)$$

where the superscript s is used to denote the incoming state is parallel or antiparallel to the local spin quantization axis of injection lead, which is very helpful, e.g. in ferromagnet we can distinguish the contribution to the total torques from the majority spin or minority spin. Such definition consists with those in Ref.[11], where an-

alytic analysis shows that for STT defined in this way equals to the exchange torques acted on the injected spin defined in Eq.(26) with only a sign difference. After summation over 2D BZ, spin torque acted on \mathbf{R} th atom can be expressed as

E. Spin current and spin torque

where the bias is given by the difference between the electrochemical potentials of the two leads as $eV_b = \mu_L - \mu_R$, and N_{\parallel} is the number of \mathbf{k}_{\parallel} points in 2D BZ.

The spin current is defined similar to the particle current in Section II.D. Considering a quasi one-dimensional TB mode for a special \mathbf{k}_{\parallel} vector, the spin density operator at site \mathbf{R} can be defined as

$$\hat{\mathbf{S}}_{\mathbf{R}}^{\mathbf{k}_{\parallel}} \equiv \sum_{L\zeta} |\mathbf{R}L\zeta^{\mathbf{k}_{\parallel}}\rangle \hat{\sigma} \langle \mathbf{R}L\zeta^{\mathbf{k}_{\parallel}}|, \quad (26)$$

where $\hat{\sigma}$ is 2×2 Pauli spin matrix. The spin current operator generally can be defined as

$$\hat{\mathcal{J}} \equiv \frac{1}{2} \left[\hat{\sigma} \otimes \hat{\mathbf{V}} + \hat{\mathbf{V}} \otimes \hat{\sigma} \right]. \quad (27)$$

note that $\hat{\mathcal{J}}$ is a tensor. For spin current between \mathbf{R} th and \mathbf{R}' th site ($\mathbf{R} \neq \mathbf{R}'$), we could project $\hat{\mathcal{J}}$ along the direction vector $\mathbf{x}_{\mathbf{R},\mathbf{R}'}$ in real space as $\hat{\mathcal{J}} \cdot \mathbf{x}_{\mathbf{R},\mathbf{R}'}$. Then the spin current operator $\hat{\mathcal{J}}_{\mathbf{R}',\mathbf{R}}(\mathbf{k}_{\parallel})$ from \mathbf{R}' th to \mathbf{R} th site ($\mathbf{R} \neq \mathbf{R}'$) can be written as

$$\hat{\mathcal{J}}_{\mathbf{R}',\mathbf{R}}(\mathbf{k}_{\parallel}) = \sum_{LL'} \frac{1}{2i\hbar} [\hat{\sigma} \hat{\mathbf{H}}_{\mathbf{R}L,\mathbf{R}'L'}^{\mathbf{k}_{\parallel}} + \hat{\mathbf{H}}_{\mathbf{R}L,\mathbf{R}'L'}^{\mathbf{k}_{\parallel}} \hat{\sigma} - h.c.]. \quad (28)$$

where $\hat{\mathcal{J}}_{\mathbf{R}',\mathbf{R}}(\mathbf{k}_{\parallel})$ is a vector only in spin space.

For a specific state $|\Psi\rangle$, the expectation value is

$$\mathbf{T}_{\mathbf{R}} = \left(\frac{\hbar}{2} \right) \frac{e}{h} \frac{1}{N_{\parallel}} \sum_{s,\mathbf{k}_{\parallel}} \langle \hat{\mathbf{T}}_{\mathbf{R}}^s(\mathbf{k}_{\parallel}) \rangle V_b, \quad (31)$$

where the bias is given by the difference between the electrochemical potentials of the two leads as $eV_b = \mu_L - \mu_R$.

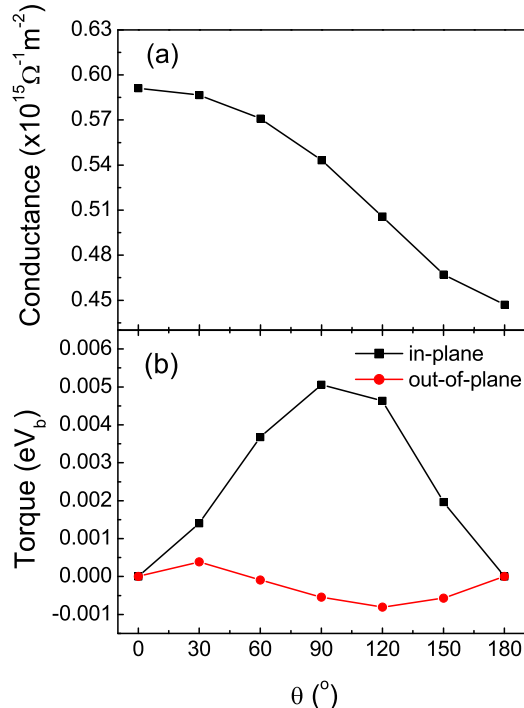


FIG. 3: (color online) (a) The total conductance of $\text{Co}(\theta)|\text{Cu}(9\text{ML})|\text{Co}(15\text{ML})|\text{Cu}$ versus polarization direction θ of fixed magnet Co. (b) The angular dependence of total spin torques on free magnet Co, where the electron current flow from the fixed magnet to the free magnet.

III. SPIN TRANSFER TORQUES IN CO/CU/FM/CU (111) SPIN VALVES

A. Ordered interfaces

A spin valve of $\text{Co}|\text{Cu}|\text{FM}|\text{Cu}$ as shown in Fig.1 is used as an example to illustrate our method. The left lead consists of semi-infinite Co with the polarization direction θ (see Fig.1). Cu spacer of 9 monolayer (ML) is located between fixed magnet Co and free magnet FM. The free magnet contains d ML, which could be Co, Ni, or $\text{Ni}_{80}\text{Fe}_{20}$ in this study. The lattice constants is assumed to be uniform in the whole spin valve, that is, $a_{\text{Cu}} = a_{\text{FM}} = 3.54 \text{ \AA}$ and the transport is along $fcc[111]$. With spd -basis, exchange-correlation potential is calculated and parameterized by Vosko-Wilk-Nusair²⁵. Our calculation gives the magnetic moments as $1.64\mu_B/\text{Co}$ atom, $2.60\mu_B/\text{Fe}$ atom and $0.62\mu_B/\text{Ni}$ atom. For the calculation of transport, total 90000 \mathbf{k}_{\parallel} points in 2D BZ are summed.

Firstly, we present the angular dependence of total conductance $G(\theta)$ of the spin valve with the free magnet to be 15ML Co in Fig.3 (a). The monotonic decrease with increase of θ is consistent with the previous *ab.initio* results¹¹. Giant magnetoresistance (GMR) can

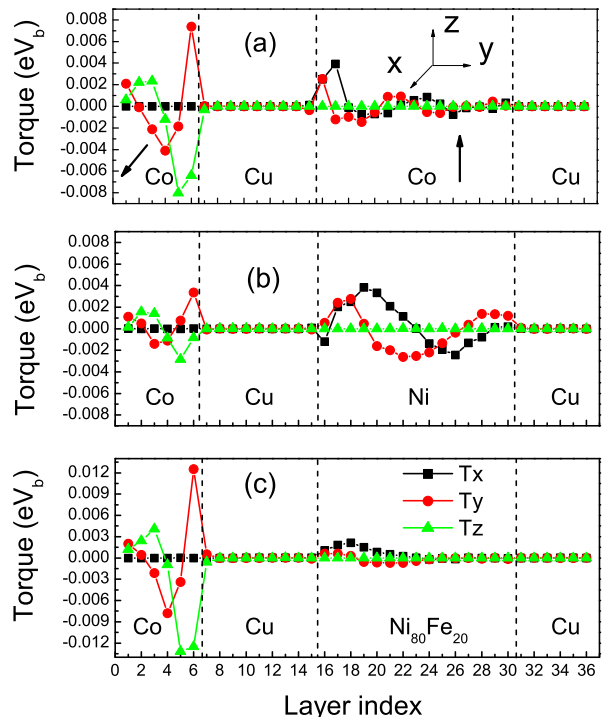


FIG. 4: (color online) The layer dependence of STT on interfacial unit cell in the spin valve $\text{Co}(\theta = 90^\circ)|\text{Cu}|\text{FM}|\text{Cu}$, where the free magnet FM are Co, Ni, $\text{Ni}_{80}\text{Fe}_{20}$ respectively.

be defined as $GMR \equiv \frac{G(0^\circ) - G(180^\circ)}{G(180^\circ)} 100\%$, which is 24% in this case. With electron current flowing from the fixed magnet to the free magnet, Fig.3 (b) gives the angular dependence of total spin torques on the free magnet Co, which restore the line shape of spin torques obtained in previous work¹¹. With the drive of the in-plane torque, magnetization of free layer is going to parallel to that of fixed layer. Due to the breakdown of time reverse symmetry for spin current, if the direction of electron current is reversed, the in-plane torques is going to drive free layer to antiparallel to fixed layer. Such phenomenon is exactly the current induced switching of magnetization observed in spin valve.

Layer resolved Spin Torque: The layer resolved STT contains the information about whether the spin angle moment is absorbed near the interface or not. Fig.4 gives the comparison of the layer dependence of STT in the spin valves with three different free magnet. Here the polarization of the fixed magnet Co is set to $\theta = 90^\circ$ without loss of generality. In our frame, \mathbf{T}_x corresponds to the in-plane torques and \mathbf{T}_y corresponds to the out-of-plane torque. The decay and oscillation of the STT are greatly different among those materials we studied. When free magnet is Co as shown in Fig.4(a), our result almost reproduces the previous result^{10,11}. The fast decay of the STT indicated the surface atoms absorbed most of the spin angle moment as the current passes by.

However, when Ni serves as the free magnet as shown in Fig.4(b), the maximum torques is not on the surface

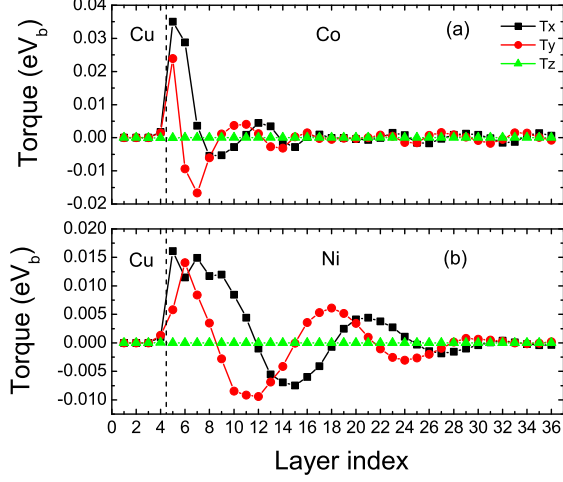


FIG. 5: (color online) The layer dependence of STT on interfacial unit cell for the spin injection setup of single interface. (a) Cu|Co (b)Cu|Ni.

atom and the decay is very slow with much longer oscillation. This observation is quite different with our previous knowledge¹⁴. The similar behavior is also found in Fig.4(c) as Ni₈₀Fe₂₀ is free magnet, the oscillation looks like that in Ni, but decaying faster. Due to the lack of obvious oscillation, the total in-plane torques on Ni₈₀Fe₂₀ ($7.7 \times 10^{-3} eV_b$) is greater than that on Co ($5.0 \times 10^{-3} eV_b$) and that on Ni ($6.3 \times 10^{-3} eV_b$).

The layer resolved STT shown in Fig.4 could be affected by the multiple scattering between the two interfaces with Cu. To remove multiple scattering effect on the torque, we perform the calculation for single interfaces of Cu(90°)|Co and Cu(90°)|Ni, with 100% polarized electrons injected from Cu side. Here Cu(90°) indicates the polarization direction of the injected electrons. The results are shown in Fig.5. For both interfaces, the maximum torques exists on the surface atoms and the oscillation spectra in ferromagnet become smoother and clear. Still the oscillation behavior strongly depends on the materials. The STT exists only near the Cu|Co interface, while the STT penetrates deep into the Ni for Cu|Ni interface. Due to the long penetration length, the multiple scattering between two Cu|Ni interface does appear in Fig.4(b).

Simple Model for Spin Torques in FM: For the layered system such as spin valve, the incoming state of the injection lead can be labelled by \mathbf{k}_{\parallel} in 2D BZ. Generally, these states will be coupled to the propagating states and evanescent states of another side of the injection interface. The STT can be expressed as

$$\Gamma \propto \sum_{\mu, \nu} C_{\mu\nu} e^{i((k_{\mu}^{\downarrow} - k_{\nu}^{\uparrow})x + \varphi_{\mu\nu})} + \mathfrak{S}_{decay}(x), \quad (32)$$

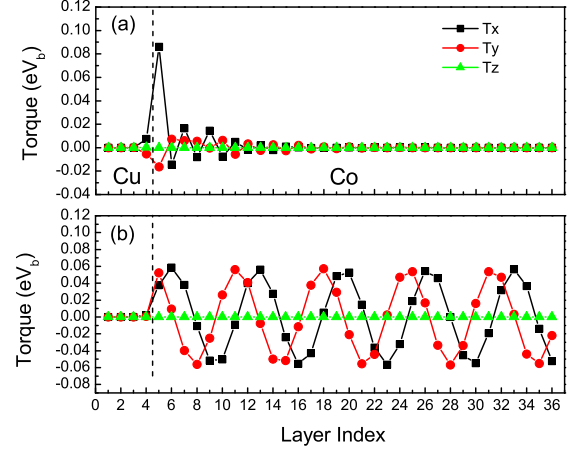


FIG. 6: (color online) (a) and (b) The layer dependence of STT on interfacial unit cell when the spin injected through a single Cu|Co interface for different \mathbf{k}_{\parallel} points in 2D BZ.

where first term denotes the contribution from the propagating states⁹ and $k_{\mu}^{\downarrow} - k_{\nu}^{\uparrow}$ gives the spatial precession frequency $\Delta k_{\mu\nu}$. The contribution from the propagating states should oscillate as function of position and will not decay as shown in Fig.6(b). However, the frequency could be quite different as \mathbf{k}_{\parallel} runs over the 2DBZ, so the final contribution will decay after summation over 2DBZ. The second term of Eq. (32), $\mathfrak{S}_{decay}(x)$, is the contribution from the evanescent states. As we have known that no particle current can be carried by evanescent state, however, such states do give effect on the spin current and also on the STT. Evanescent states do contribute to spin torques and should responds for the initio decay of the STT in the system as Co|Cu|Co|Cu, as shown in Fig.6(a) where the evanescent state dominates.

Two reasons could account for the decay of the STT away from the interface. (i) Vanishing of the evanescent states' contribution. For Cu|Co, our calculation shows that this part of contribution is about 10% of the total torques on the first layer close to injection interface. (ii) Cancellation effect among different \mathbf{k}_{\parallel} in 2D BZ⁹.

The materials dependency of the STT could be understood based on the Fermi surface of Ni and Co. The wave vector $k_{\mu(\nu)}^{\downarrow(\uparrow)}$ can be found by the projection of minority spin (majority spin) Fermi surface of ferromagnet along the current direction, where μ (ν) denotes the different sheets of Fermi surface for minority spin (majority spin). In Fig.7, the Fermi surface for Co and Ni viewed along the (111) direction for majority and minority spins is shown. As the shape of Fermi surface for majority spin and minority spin in Co are greatly different to each other, the precession frequencies $\Delta k_{\mu\nu}$ of injected spin are varied rapidly as \mathbf{k}_{\parallel} running over the 2DBZ. After summation of 2D BZ, the strong cancellation is expected as shown in Fig.4(a) and Fig.5(a). However, for Cu|Ni, due to

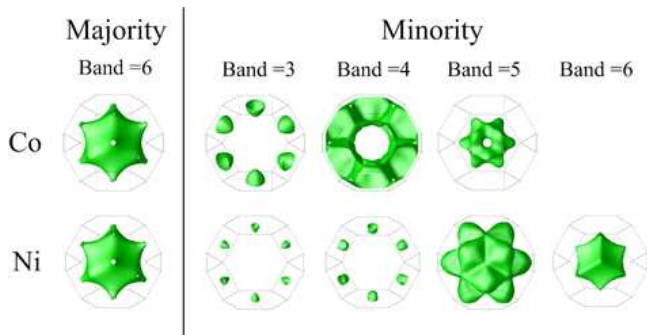


FIG. 7: (color online) The First row: Fermi surface projection of the Co bulk fcc Brillouin zone on to a plane perpendicular the (111) direction. Left-hand panel is for majority electron and right-hand panel is for minority electron with band 3,4,5 FS. The Second row is Ni bulk.

the similar symmetry between the wave function of the sheet $\mu = 6$ of minority spin and that of Cu, the electrons pass Cu|Ni interface mainly through this channel ($\mu = 6$). While for majority spin, the Fermi surface contains only one sheet. The precession frequency is dominated by Δk_{66} . Similar shape of sheet $\mu = 6$ of minority spin and sheet $\nu = 6$ of majority spin will result in amount of propagating states with similar precession frequency. After summation of those states, the cancellation could be weak and collective oscillation must be of long period.

The above physical picture about spin torques in FM should be qualitatively applicable to the system with FM to be $\text{Ni}_{80}\text{Fe}_{20}$. For $\text{Ni}_{80}\text{Fe}_{20}$, the overall band structure resembles that of Ni, however, due to the scattering of Fe impurity atoms, the fine structure at Fermi surface could be much more complicated than that of Ni. The dispersion of precession frequency $\Delta k_{\mu\nu}$ is large and the cancellation should be strong. As a result, the decay of spin torque is much faster than in the conventional FM, Ni and Co. Besides, spin-orbit coupling is not included in our calculation yet, which could introduce new mechanism of decay in $\text{Ni}_{80}\text{Fe}_{20}$.

B. Interfacial disorder

Interfacial disorder is likely to exist in the metallic system. Previous studies¹⁷ showed that the interfacial alloy could change the polarization of the interface resistance. How the interfacial disorder affects the STT is question we would like to answer in this section. The interfacial disorder is introduced by two layers of substitutional alloy $\text{Cu}_x\text{FM}_{1-x}$ and $\text{Cu}_{1-x}\text{FM}_x$ at interface between Cu and FM. In present study, alloy is modelled by a 8×8 lateral supercell, which was shown to be a good modelling of the interfacial alloy¹⁷.

In Fig.8(a)&(b), the concentration x dependence of total conductance and total torque (in-plane and out-of-plane) on free magnet are given for the realistic spin valve of $\text{Co}(\theta = 90^\circ)|\text{Cu}|\text{Co}(\text{Ni})|\text{Cu}$. The total conductance de-

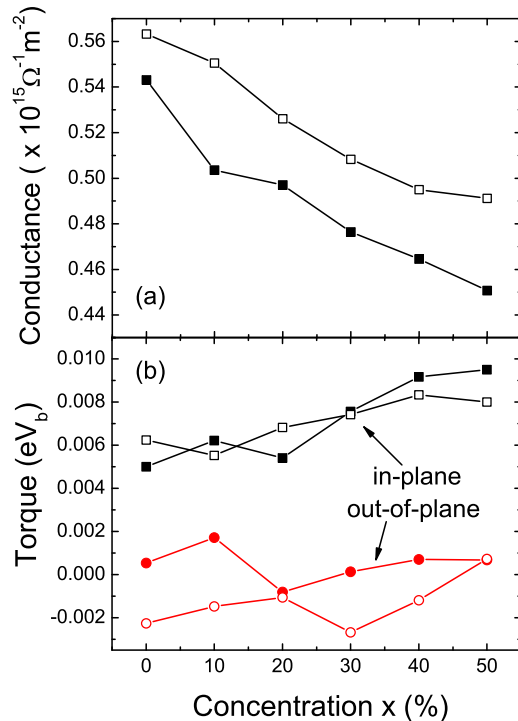


FIG. 8: (color online) The concentration x dependence of the conductance (a) and total spin torques on the free magnet (b) of spin valve $\text{Co}(\theta = 90^\circ)|\text{Cu}|\text{FM}|\text{Cu}$ with interfacial alloy $\text{Cu}_x\text{FM}_{1-x}$, where the solid symbol for FM to be Co and open symbol for FM to be Ni. In (b), the black symbol for in-plane torques and red symbol for out-of-plane torque.

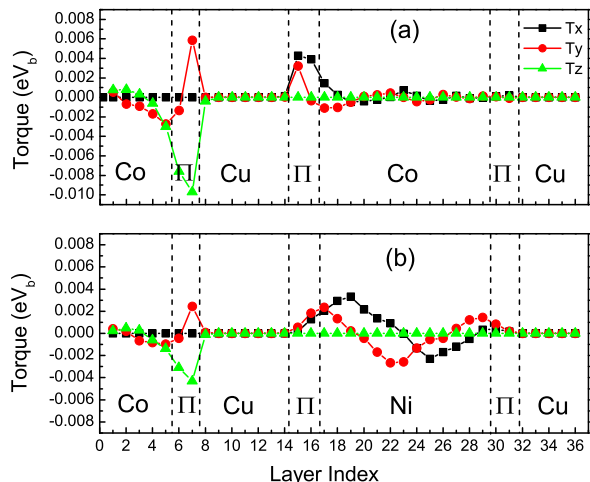


FIG. 9: (color online) The layer dependence of STT on interfacial unit cell in the spin valve $\text{Co}(\theta = 90^\circ)|\text{Cu}|\text{FM}|\text{Cu}$ with interfacial disorder, (a) FM is Co, (b) FM is Ni. The zone labelled by Π is the layers with substitutional alloy $\text{Cu}_{50}\text{FM}_{50}$.

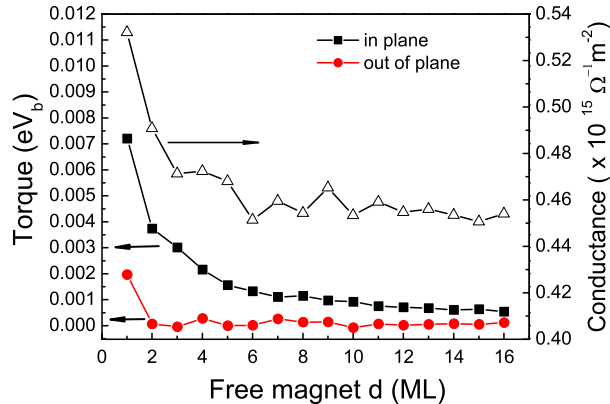


FIG. 10: (color online) The thickness d dependence of the averaged spin torques on the atom in free magnet and the total conductance of the spin valve.

creases with increase of the concentration x , which means the interfacial disorder will suppress electronic transport in this system. However, as shown in Fig.8(b), the total in-plane torques acted on free magnet increase when the disorder is enhanced in spite of the almost constant out-of-plane spin torque. The increase is around 50% for Co and 30% for Ni.

In Fig.9, the layer dependence of spin torques is shown. Comparing with Fig.4(a), it is found that the torques on atoms near the interface with Cu spacer have been enhanced. This result means that the interfacial roughness will not kill the interfacial spin torques, on the contrary, the dirty interface may be helpful to enhance the torques transfer.

For the spin valve with FM is Co, the free magnet thickness d dependence of the total conductance and STT

are shown in Fig.10, where the spin torques is obtained by average of total torques on free magnet over all atoms in free magnet. Due to the quantum size effect, the conductance decays with a small oscillation and tend to be constant with increase of free magnet thickness. The in-plane torques dominates over the out-of-plane torques for all thickness.

IV. SUMMARY

Based on the first principles frame, a method was developed to calculate the transport and spin torques of the layered system with noncollinear magnetization in linear response regime. STT in the ferromagnetic (FM) spin valves are calculated. We found that the behavior of spin torques in the free layer are greatly dependent on the materials. The cancellation effect of the STT due to the different precessional frequency is sensitive to the band structure of material. The contribution of evanescent states to the STT is found to be nontrivial at the NM|FM interface. The effect due to interfacial disorder is also considered, it is found that average torques are enhanced in the presence of disorder.

Acknowledgments

This work is supported by NSF(10634070) and MOST(2006CB933000, 2006AA03Z402) of China. We are grateful to: Paul Kelly for useful discussion; Ilja Turek for his TB-LMTO-SGF layer code which we used to generate self-consistent potentials; Anton Starikov for permission to use his version of the TB-MTO code based upon sparse matrix techniques with which we can solve Eq.(15) in an efficient way.

-
- ¹ J. Slonczewski, J. Magn. Magn. Mater. **159**, L1 (1996).
 - ² L. Berger, Phys. Rev. B **54**, 9353 (1996).
 - ³ M. Tsoi, A. G. M. Jansen, J. Bass, W. -C. Chiang, M. Seck, V. Tsoi, and P. Wyder, Phys. Rev. Lett. **80**, 4281 (1998); M. Tsoi, A. G. M. Jansen, J. Bass, W. -C. Chiang, V. Tsoi, and P. Wyder, Nature (London) **406**, 46 (2000); E. B. Myers, D. C. Ralph, J. A. Katine, R. N. Louie, and R. A. Buhrman, Science **285**, 867 (1999).
 - ⁴ J. Z. Sun, Phys. Rev. B **62**, 570 (2000).
 - ⁵ Y. B. Bazaliy, B. A. Jones, and S. -C. Zhang, Phys. Rev. B **57**, R3213 (1998).
 - ⁶ X. Waintal, E. B. Myers, P. W. Brouwer, and D. C. Ralph, Phys. Rev. B **62**, 12317 (2000).
 - ⁷ A. Brataas, Yu. V. Nazarov, and Gerrit E. W. Bauer, Phys. Rev. Lett. **84**, 2481 (2000); Eur. Phys. J. B **22**, 99 (2001).
 - ⁸ M. D. Stiles, A. Zangwill, J. Appl. Phys. **91**, 6812 (2002).
 - ⁹ M. D. Stiles, A. Zangwill, Phys. Rev. B **66**, 014407 (2002).
 - ¹⁰ D. M. Edwards, F. Federici, J. Mathon, A. Umerski, Phys. Rev. B **71**, 054407 (2005).
 - ¹¹ P. M. Haney, D. Waldron, R. A. Duine, A. S. Núñez, H. Guo, and A. H. MacDonald, Phys. Rev. B **76**, 024404 (2007).
 - ¹² G. D. Fuchs, J. A. Katine, S. I. Kiselev, D. Mauri, K. S. Wooley, D. C. Ralph, and R. A. Buhrman, Phys. Rev. Lett. **96**, 186603 (2006); Hao Meng, Jianguo Wang, and Jian-Ping Wang, Appl. Phys. Lett. **88**, 082504 (2006).
 - ¹³ Masamitsu Hayashi, Luc Thomas, Charles Rettner, Rai Moriya, Yaroslav B. Bazaliy, and Stuart S. P. Parkin, Phys. Rev. Lett. **98**, 037204(2007); M. Yamanouchi, D. Chiba, F. Matsukura, T. Dietl, and H. Ohno, Phys. Rev. Lett. **96**, 096601(2006).
 - ¹⁴ Maciej Zwierzycki, Yaroslav Tserkovnyak, Paul J. Kelly, Arne Brataas, and Gerrit E. W. Bauer, Phys. Rev. B **71**, 064420 (2005).
 - ¹⁵ K. Carva and I. Turek, Phys. Rev. B **76**, 104409 (2007).
 - ¹⁶ J. Bass and W. P. Pratt Jr., J. Magn. Magn. Mater. **200**,

- 274 (1999).
- ¹⁷ K. Xia, M. Zwierzycki, M. Talanana, P. J. Kelly, and G. E. W. Bauer, Phys. Rev. B **73**, 064420 (2006).
- ¹⁸ Yuan Xu, Shuai Wang, and Ke Xia, arXiv:0708.2143v1.
- ¹⁹ I. Turek, V. Drchal, J. Kudrnovský, M. Šob, and P. Weinberger, *Electronic Structure of Disordered Alloys, Surfaces and Interfaces* (Kluwer, Boston-London-Dordrecht, 1997).
- ²⁰ J. Kudrnovský, V. Drchal, C. Blaas, P. Weinberger, I. Turek, and P. Bruno, Phys. Rev. B **62**, 15084 (2000).
- ²¹ O. K. Andersen, O. Jepsen, and D. Glözel, in *Highlights of Condensed Matter Theory*, edited by F. Bassani, F. Fumi and M. P. Tosi (North-Holland, Amsterdam, 1985), pp. 59-176.
- ²² T. Ando, Phys. Rev. B **44**, 8017 (1991).
- ²³ I. Turek, J. Kudrnovský, V. Drchal, L. Szunyogh, and P. Weinberger, Phys. Rev. B **65**, 125101 (2002).
- ²⁴ S. Datta, *Electronic Transport in Mesoscopic Systems* (Cambridge University Press, Cambridge, 1995).
- ²⁵ S. H. Vosko, L. Wilk, and M. Nusair, Can. J. Phys. **58**, 1200 (1980).